

# Coexistence of charge density waves, bond order waves and spin density waves in quasi-one dimensional charge transfer salts

J. Riera<sup>a,b</sup> and D. Poilblanc<sup>a</sup>

<sup>a</sup>*Instituto de Física Rosario, Consejo Nacional de Investigaciones Científicas y Técnicas, y Departamento de Física, Universidad Nacional de Rosario, Avenida Pellegrini 250, 2000-Rosario, Argentina*

<sup>b</sup>*Laboratoire de Physique Quantique & UMR-CNRS 5626, Université Paul Sabatier, F-31062 Toulouse, France*  
(December 2, 2024)

Charge, spin, as well as lattice instabilities are investigated in isolated or weakly coupled chains of correlated electrons at quarter-filling. Our analysis is based on extended Hubbard models including nearest neighbor repulsion and Peierls coupling to lattice degrees of freedom. While treating the electronic quantum fluctuations exactly, the lattice structure is optimized self-consistently. We show that, generically, isolated chains undergo instabilities towards coexisting charge density waves (CDW) and bond order waves (BOW) insulating phases. The spin and charge gaps of the BOW-CDW phase are computed. In the presence of an interchain magnetic coupling spin density waves phases including a CDW or a BOW component are also found. Our results are discussed in the context of insulating charge transfer salts.

PACS: 75.10.-b, 75.50.Ee, 71.27.+a, 75.40.Mg

Quasi-one dimensional correlated electrons systems at quarter-filling show fascinating physical properties. A widely studied class of such materials are the so-called organic charge transfer salts like the Bechgaard salts  $(\text{TMTSF})_2\text{X}$  or their sulfur analogs  $(\text{TMTTF})_2\text{X}$  ( $\text{X}=\text{PF}_6, \text{AsF}_6$ ) [1–3]. These systems which consist of stacks of organics molecules forming weakly coupled one dimensional (1D) chains exhibit, at low temperature, a large variety of exotic phases such as triplet superconducting [4], spin density wave (SDW), charge density wave (CDW) and spin-Peierls (SP) phases [5]. The compounds of the sulfur  $(\text{TMTTF})_2\text{X}$  series show strong charge localization at rather high temperature  $T_\rho$  (as signalled e.g. by transport measurements) as well as a weak (to moderate) dimerization along the stacks [1,2]. The insulating behavior observed in this regime has been interpreted as 1D CDW fluctuations [3] or using a Hubbard chain Hamiltonian with an explicit dimerization [6]. At a significantly lower temperature  $T_{SP}$  (typically  $T_{SP} \sim 15\text{K}$ ) a SP transition occurs together with a tetramerization along the chains [1,5]. In this system the interplay between charge ordering and lattice instability is poorly understood. In particular whether the tetramerization (connected to the spin gap) is occurring simultaneously with a CDW transition is still controversial. So far the existing theory of the SP phase [7] do not consider the possibility of a coexisting  $2k_F$  CDW. Interestingly enough, CDW fluctuations were seen by X-ray diffuse scattering [8] in the SDW phase of the (more metallic)  $(\text{TMTSF})_2\text{PF}_6$  compound.

In this paper, our aim is to investigate by numerical exact diagonalization (ED) techniques, the interplay between the electron repulsion and the electron-phonon coupling in the case of an adiabatic lattice [9]. We focus on the competition or the cooperative behavior between charge ordering and lattice instabilities. Such a problem has been addressed in a number of previous stud-

ies [10,11] where several interesting modulated phases have been proposed. However, so far, no systematic investigation of the full phase diagrams has been carried out. Indeed, the suggested translation symmetry broken states [11] were found in a restricted variational space. We shall here re-examine these issues in order to determine the absolute stability of the various competing phases.

We use extended 1D Hubbard models at quarter-filling ( $\bar{n} = 1/2$ ) coupled with some (classical) phonon field,

$$H_{1D} = \sum_{i,\sigma} t(i)(c_{i;\sigma}^\dagger c_{i+1;\sigma} + h.c.) + U \sum_i n_{i;\uparrow} n_{i;\downarrow} + V \sum_i n_i n_{i+1} + H_{\text{ph}}, \quad (1)$$

where  $n_{i;\sigma} = c_{i;\sigma}^\dagger c_{i;\sigma}$  and  $n_i = n_{i;\uparrow} + n_{i;\downarrow}$ . We have included a nearest neighbor (NN) interaction  $V$  as its role will become clear in the following. Local deformations of the molecules can produce changes of the on-site (or molecular) orbitals energies and can simply be taken into account by a Holstein term  $\sum_i n_i \delta_i$  while assuming a constant hopping integral  $t(i) = t$  and an elastic energy cost  $\frac{1}{2}K \sum_i \delta_i^2$ . This effect has been studied numerically in a different context [12] but it is relatively small in the case of the organic systems we are considering here. Therefore, we shall only discuss it briefly later on. In contrast to the above on-site deformation, the positions of the intercalated anions can couple strongly to the electrons especially through modulations of the single particle hoppings along the chains. To mimic this effect we assume a Peierls coupling of the form

$$t(i) = t(1 + \delta_i^B) \quad (2)$$

with an elastic energy

$$H_{\text{ph}} \equiv H_{\text{elas}} = \frac{1}{2}K_B \sum_i (\delta_i^B)^2. \quad (3)$$

Note that the electron-lattice couplings have been absorbed in the re-definition of the displacements  $\delta_i^B$ . Therefore, the strength of the lattice couplings scale like the inverse of the elastic constants  $1/K_B$ . Note also that energies are measured in unit of  $t$ . First, we shall consider the case of the *isolated* Hubbard chain in the presence of the Peierls coupling. Next, the role of an inter-chain magnetic coupling (in mean field) will be considered.

In contrast to previous treatments [11] our numerical method enable us to obtain the lowest energy equilibrium lattice configuration without making any assumption on the broken symmetry ground state (GS). In particular, no super-cell order is imposed *a priori* and the GS configuration is obtained through a self-consistent procedure. Indeed, the total energy functionals  $E(\{\delta_i^B\})$  can be minimized with respect to the sets of distortions  $\{\delta_i^B\}$  by solving the following non-linear coupled equations,

$$K_B \delta_i^B + t \langle c_{i;\sigma}^\dagger c_{i+1;\sigma} + h.c. \rangle = 0. \quad (4)$$

Here  $\langle \dots \rangle$  is the GS mean value obtained by ED (using the Lanczos algorithm) of Hamiltonian (1) on cyclic  $L$ -site rings (with  $L$  up to 16 sites). Since the second term depends implicitly on the distortion pattern  $\{\delta_i^B\}$ , Eq. (4) can be solved by a regular iterative procedure [13]. A similar approach has been applied to the case of the on-site Holstein coupling [12].

Before discussing our main results on the Hubbard-Peierls chain, let us briefly describe the phase diagram of the Hubbard-Holstein chain [12] in order to introduce the generic types of CDW states. At quarter-filling, the Fermi wave vector is given by  $q_{2k_F} = \frac{\pi}{2}$  so that, at small  $U$ , one expects an instability towards a  $2k_F$  CDW state of wavevector  $\lambda_{2k_F} = 4a$  ( $a$  is the lattice spacing) mediated by the electron-lattice coupling. In contrast, for large  $U$ , the system becomes more similar to a gas of interacting spinless fermions (SF) and the instability is likely to occur at wavevector  $2k_F^{SF} = 4k_F$ . More generally, we can parameterize the relative charge density modulation as,

$$\frac{\Delta n_i}{\bar{n}} = \rho_{4k_F} \cos(2\pi \frac{r_i}{2a}) + \rho_{2k_F} \cos(2\pi \frac{r_i}{4a} + \Phi_{2k_F}), \quad (5)$$

where  $\Delta n_i = \langle n_i \rangle - \bar{n}$ . Complete phase diagrams of the Hubbard-Holstein chain have been established in Ref. [12] and we briefly summarize them here. For  $V = 0$  the metallic uniform U phase ( $\rho_{2k_F} = \rho_{4k_F} = 0$ ) is restricted to a region at small lattice coupling. Above a critical line  $(1/K)_U$ , three different insulating CDW phases can be distinguished; (i) at small  $U$ , a  $2k_F$  CDW phase ( $\rho_{4k_F} = 0$ ) centered on the sites, i.e. with  $\Phi_{2k_F} = 0$ ; (ii) at intermediate  $U$  (in the range 4-8), a *bond-centered*  $2k_F$  CDW phase (i.e. with  $\Phi_{2k_F} = \frac{\pi}{4}$ ); (iii) at large  $U$ , a  $4k_F$  CDW ( $\rho_{2k_F} = 0$ ). As discussed in Ref. [12], a small NN repulsion suppresses completely the intermediate phase and enlarges the region of stability of the  $4k_F$  CDW phase. Although these CDW might have some relevance to the low temperature phase of the (TMTTF)<sub>2</sub>X family, their charge modulations should couple strongly

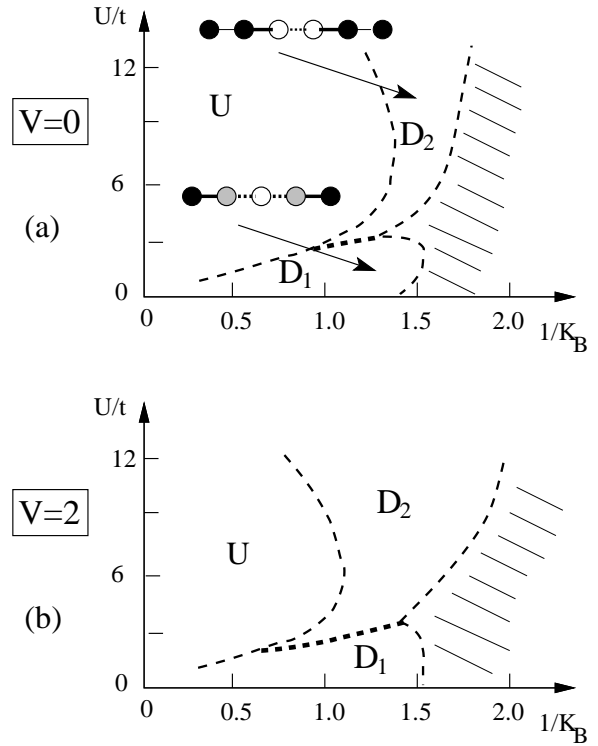


FIG. 1. Typical  $(U/t, 1/K_B)$  phase diagrams of a  $\frac{1}{4}$ -filled Hubbard-Peierls chain without (a) or with a nearest neighbor Coulomb repulsion  $V$  (b) obtained from ED of small periodic chains. Hashed regions are unphysical.

to the anion potential. Therefore, we investigate next the role of a Peierls coupling.

The phase diagrams as a function of the on-site repulsion  $U/t$  and the Peierls coupling  $1/K_B$  are shown in Figs. 1(a,b) for  $V = 0$  and  $V = 2$ . For too large electron-lattice coupling the linear coupling approximation breaks down and our model becomes unphysical (hashed regions) so that we shall restrict to small and intermediate values of  $1/K_B$ . For intermediate values of  $1/K_B$ , the uniform state is unstable towards translation symmetry broken states. Such bond order wave (BOW) states are characterized by a modulation of the hopping amplitudes of the form,

$$\delta_i^B = \delta_{4k_F}^B \cos(2\pi \frac{r_i}{2a}) + \delta_{2k_F}^B \cos(2\pi \frac{r_i}{4a} + \Phi_{2k_F}^B). \quad (6)$$

Generically, we find that BOW coexist with weaker charge modulations (CDW) given by (5). The amplitudes of the bond and charge modulations are shown in Fig. 2(a) for a fixed electron-lattice coupling  $K_B = 0.8$ . Very small finite size effects are observed and calculations on 12- and 16-site rings give almost identical results. Two different types of structures are stable; (i) in the weak coupling regime (let's say  $U/t < 3$ ), a strong  $2k_F$  BOW with  $\Phi_{2k_F}^B = \pi/4$  i.e. corresponding to a X-

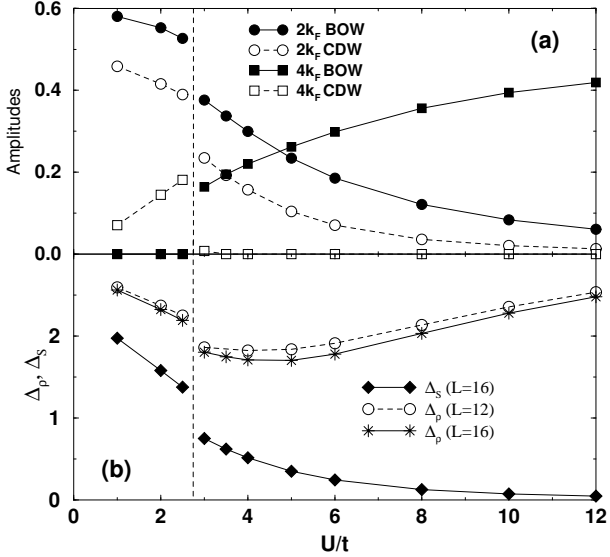


FIG. 2. (a) Amplitudes of the CDW ( $\rho_{2k_F}$  &  $\rho_{4k_F}$ ) and BOW ( $\delta_{2k_F}^B$  &  $\delta_{4k_F}^B$ ) components versus  $U/t$  for  $(K_B)^{-1} = 1.25$  and  $V = 2$  (computed on a 16-site ring). Open (close) symbols correspond to CDW (BOW). Note that, although identical symbols have been used, the  $2k_F$  orders are in fact *different* (i.e. have different phases  $\Phi_{2k_F}$  and  $\Phi_{2k_F}^B$ ) in the small- ( $D_1$ ) and large- $U$  ( $D_2$ ) phases (see text). (b) Charge ( $\Delta_\rho$ ) and spin ( $\Delta_S$ ) gaps in unit of  $t$  vs  $U/t$  computed on 12- and 16-site rings ( $\Delta_S$  on  $L = 12$  and  $L = 16$  are undistinguishable).

X–Y–Y type of sequence of the bonds occurs. This modulation coexists with a weaker  $2k_F$  site-centered CDW (A–B– $\bar{A}$ –B type of sequence of the on-site charge densities, A and  $\bar{A}$  corresponding to opposite values of  $\Delta n_i$ ) and an even weaker  $4k_F$  (i.e. A–B–A–B) CDW component ( $D_1$  phase); (ii) at larger  $U/t$ , the  $D_2$  phase corresponds to the superposition of a lattice dimerization ( $4k_F$  BOW) together with a tetramerization ( $2k_F$  BOW with  $\Phi_{2k_F}^B = 0$ ). In other words, among the, let's say, weak bonds of the dimerized state, one every two becomes weaker (or stronger) so that electrons become weakly bound in singlet pairs on next NN bonds. The  $D_2$  phase is therefore a simple realization of the above mentioned SP phase. Interestingly enough, we observe that the tetramerization leads to a weak coexisting  $2k_F$  CDW component correspond to a A–A–B–B charge modulation (i.e. with  $\Phi_{2k_F} = \pi/4$ ). Note also that the boundary between the  $D_1$  and  $D_2$  phases is a first-order transition line as it is clear from the discontinuity of the various order parameters seen in Fig. 2(a).

To complete our study we have also computed the charge ( $\Delta_\rho$ ) and the spin ( $\Delta_S$ ) gaps in the  $D_1$  and  $D_2$  phases for the same set of parameters as shown in Fig. 2(b). As for the Fourier amplitudes, finite size effects are almost negligible especially for  $\Delta_S$ . Clearly  $\Delta_S$

follows closely the magnitude of the  $2k_F$  BOW-CDW. For large- $U$  (and large dimerization) the system behaves qualitatively like a spin-1/2 antiferromagnet (since the electrons are localized on the strong bonds) and the spin gap is expected to vanish in this limit. In contrast, in the  $D_1$  phase, electrons are strongly localized in pairs on 2 adjacent strong bonds (i.e. on 3 sites) so that  $\Delta_S \sim t$ . The charge gap, also shown in Fig. 2, has a minimum at intermediate  $U$  in the region corresponding to the crossover from dominant  $2k_F$  to dominant  $4k_F$  BOW-CDW. Note that both charge and spin gaps are discontinuous at the first order transition between  $D_1$  and  $D_2$ .

Our study shows that the electronic correlations (both  $U$  and  $V$ ) are essential to stabilize the  $D_2$  phase which, we believe, is a fair realization of the SP phase of the (TMTTF) $_2$ X material. Indeed, (i) the  $D_2$  phase is stable only above a critical value of  $U/t$  and (ii) the NN repulsion  $V$  enlarges significantly its range of stability. Note that the  $2k_F$  ( $4k_F$ ) Fourier components are suppressed (increased) as  $U/t$  increases as seen in Fig. 2(a).

Lastly, we investigate the role of an inter-chain coupling which is relevant e.g. in the case of (TMTTF) $_2$ Br (or (TMTTF) $_2$ PF $_6$  under pressure). These systems which are less anisotropic than (TMTTF) $_2$ PF $_6$  at ambient pressure exhibit an antiferromagnetic (AF) phase at low temperature. In an insulating regime, due to the presence of a charge gap  $\Delta_\rho$ , the inter-chain single particle hopping  $t_\perp$  is believed to be irrelevant [14,3]. Therefore, we shall only consider a transverse magnetic coupling  $J_\perp$  (typically  $J_\perp \sim t_\perp^2/\Delta_\rho$ ) in mean field approximation. Our previous method can be straightforwardly extended to include this inter-chain coupling by adding to (1) an extra term as,

$$H_\perp = \frac{1}{2} \sum_i H_i (n_{i;\uparrow} - n_{i;\downarrow}), \quad (7)$$

where the local fields  $H_i$  are determined self-consistently (simultaneously with the  $\delta_i^B$  bond modulations) from an additional set of non-linear equations,

$$H_i = \frac{J_\perp}{2} \langle (n_{i;\uparrow} - n_{i;\downarrow}) \rangle. \quad (8)$$

Our results on coupled Hubbard-Peierls chains are summarized in Fig. 3(a). Besides the  $D_2$  phase which is stable at small  $J_\perp$  new magnetic phases depicted in Figs. 4 appear; (i) at small electron-lattice coupling an antiferromagnetic phase consisting of a site-centered  $4k_F$  CDW with a finite spin density on the sites carrying an excess charge (see Fig. 4(b)); (ii) at larger values of  $1/K_B$ , a superposition of a dimerization ( $4k_F$  BOW) with a  $2k_F$  *bond-centered* SDW order [15] (see Fig. 4(c)). Note that only the spin densities of these two magnetic phases could be obtained by adding two out-of-phase  $2k_F$  CDW for the spins up and down so that the  $4k_F$  CDW and BOW components should really be considered as extra coexisting orders. Note also that, in a small region of the parameter space, a more exotic magnetic SDW $_2$  phase (not shown)

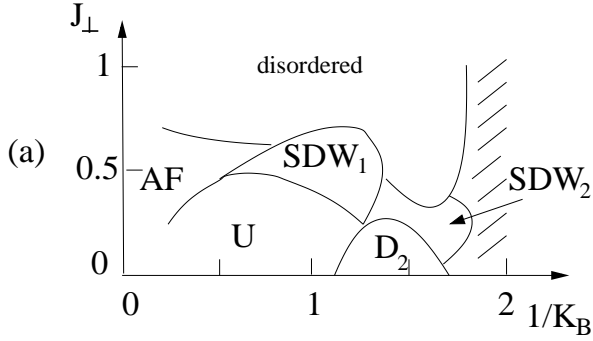


FIG. 3. Phase diagram of weakly coupled  $\frac{1}{4}$ -filled Hubbard-Peierls chains as a function of  $1/K_B$  and  $J_\perp$  for  $U=6$ ,  $V=2$ . Hashed regions are unphysical.

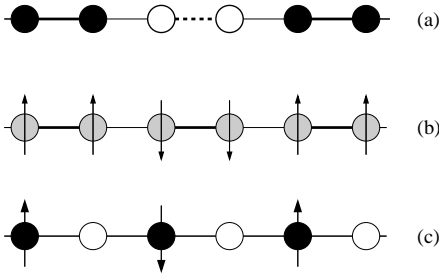


FIG. 4. Pictures of the various phases of antiferromagnetically coupled chains showing the bond modulation (thick lines are strong bonds, dashed lines are weak bonds), the charge modulation (full and open circles correspond to excess and depression of charge respectively) and the local spin densities (arrows). (a) dimerized/tetramerized  $D_2$  phase; (b) Spin density wave  $SDW_1$  phase; (c) antiferromagnetic phase.

has been stabilized on our clusters. This phase contains all three CDW, SDW and BOW components with large supercells of the order of our chain lengths. Therefore, establishing the actual stability of this phase would require larger systems.

For completeness, in addition to the extended Hubbard-Peierls model (1), we have also considered its large- $U$  version, namely a  $t$ - $J$ -Peierls model (where doubly occupied sites are projected out). We have obtained a phase diagram which is qualitatively very similar to the one of the Hubbard-Peierls model apart from the exotic  $SDW_2$  phase which is not seen in this case.

To summarize, the role of Peierls electron-lattice couplings has been investigated in the adiabatic approximation in quarter-filled isolated or weakly coupled one-dimensional Hubbard chains. A numerical method based on ED techniques supplemented by a self-consistent procedure has been used to determine the various phase diagrams as a function of the strengths of the lattice coupling and the Coulomb repulsion. We have shown that, generically, lattice modulations (BOW) are always

accompanied by CDW's of weaker amplitudes. In addition, at intermediate and large on-site Coulomb repulsion, the lattice modulation consists of a superposition of a  $4k_F$  (dimerization) and a  $2k_F$  (tetramerization) BOW. Interestingly enough, we found that a NN electronic repulsion further stabilizes this lattice/charge modulated phase. Under the application of an inter-chain AF coupling, we found new long range spin order phases showing coexisting  $4k_F$  CDW or BOW (i.e. dimerization). It is argued that such a simple model can well describe the various low temperature SP, AF and SDW phases of the insulating charge transfer salts of the sulfur series [5].

Computations were performed at the Supercomputer Computations Research Institute (SCRI) and at the Academic Computing and Network Services at Tallahassee (Florida) and at IDRIS, Orsay (France). Support from ECOS-SECyT A97E05 is also acknowledged.

- 
- [1] D. Jérôme and H. J. Schulz, *Adv. Phys.* **31**, 299 (1982); C. Bourbonnais and D. Jerome, in *Advances in Synthetic Metals, Twenty Years of Progress in Science and Technology*, edited by P. Bernier, S. Lefrant, and G. Bidan (Elsevier, New York, 1999), pp. 206-261.
  - [2] T. Ishiguro, K. Yamaji, and G. Saito, in *Organic Superconductors*, 2nd ed., Springer Series in Solid-State Sciences, Vol. 88 (Springer-Verlag, Berlin, 1998).
  - [3] C. Bourbonnais, cond-mat/0004470 preprint.
  - [4] I. J. Lee *et al.*, *Phys. Rev. Lett.* **78**, 3555 (1997).
  - [5] M. Dumm *et al.*, *Phys. Rev. B* **61**, 511 (2000) and references therein.
  - [6] Karlo Penc and Frédéric Mila, *Phys. Rev. B* **50**, 11 429 (1994).
  - [7] B. Dumoulin *et al.*, *Phys. Rev. Lett.* **76**, 1360 (1996).
  - [8] J. P. Pouget and S. Ravy, *J. Phys. I (France)* **6** 1501 (1996).
  - [9] For the treatment of non-adiabatic phonons in spin chains see e.g. D. Augier *et al.*, *Phys. Rev. B* **58**, 9110 (1998).
  - [10] K. C. Ung, S. Mazumdar and D. K. Campbell, *Solid St. Commun.*, **85**, 917 (1993); K. C. Ung, S. Mazumdar and D. Toussaint, *Phys. Rev. Lett.* **73**, 2603 (1994).
  - [11] S. Mazumdar, S. Ramasesha, R. Torsten Clay and D. K. Campbell, *Phys. Rev. Lett.* **82**, 1522 (1999); S. Mazumdar, R. T. Clay and D. K. Campbell, cond-mat/0003200 preprint.
  - [12] J. Riera and D. Poilblanc, *Phys. Rev. B* **59**, 2667 (1999).
  - [13] A. Dobry and J. Riera, *Phys. Rev. B* **56**, 2912 (1997).
  - [14] For numerical studies of the role of  $t_\perp$  on *metallic* Hubbard chains see e.g. S. Capponi, D. Poilblanc and E. Arrigoni, *Phys. Rev. B* **57**, 6360 (1998) and references therein.
  - [15] Note that these SDW Mott-insulators should not be confused with the weak coupling SDW phases of the quasi-1D (TMTSF)<sub>2</sub>X metals.